agronomy

MDPI

*Article*

# Deficit Irrigation Strategies Modulate Grape Maturation and Volatile Aroma Composition in Pinot Gris Wines

**Mirko Sodini [1], Alessandro Pichierri [1], Lara Tat [1], Piergiorgio Comuzzo [1], Amelia Caffarra [2], Selena Tomada [3], Klemen Lisjak [4], Andreja Vanzo [4] and Paolo Sivilotti [1,*]**

[1] Department of Agricultural, Food, Environmental and Animal Sciences, University of Udine, Via delle Scienze 206, 33100 Udine, Italy; mirko.sodini@uniud.it (M.S.); alessandro.pichierri@uniud.it (A.P.); lara.tat@uniud.it (L.T.); piergiorgio.comuzzo@uniud.it (P.C.)
[2] ITK, 45 All. Yves Stourdze, 34830 Clapiers, France; amelia.caffarra@itk.fr
[3] ERSA, Regional Agency for Rural Development, Via Sabbatini 5, 33050 Pozzuolo del Friuli, Italy; selena.tomada@ersa.fvg.it
[4] Department of Fruit Growing, Viticulture and Oenology, Agricultural Institute of Slovenia, Hacquetova ulica 17, 1000 Ljubljana, Slovenia; klemen.lisjak@kis.si (K.L.); andreja.vanzo@kis.si (A.V.)
* Correspondence: paolo.sivilotti@uniud.it

**Abstract**

Climate change is increasing the frequency of droughts, raising the need for sustainable irrigation management in viticulture. This study evaluated the effects of three deficit irrigation regimes—well-watered (WW), mild deficit (MiD), and moderate deficit (MoD)—implemented through the decision support system Vintel® in a Pinot gris vineyard in Friuli Venezia Giulia (Italy). Vine physiology, grape ripening, and wine aroma profile were assessed across two seasons. The water deficit treatments modulated yield parameters (specifically, cluster weight was reduced by 12% and 10% for Mid and Mod as compared to WW) and delayed sugar accumulation, particularly under MoD (9% Brix reduction as compared to WW). While basic wine composition largely reflected grape maturity, volatile aroma compounds showed variable responses to irrigation and were strongly modulated by seasonal conditions. MiD had a minimal impact on the aroma profile, whereas MoD led to reduced sugar and altered volatile composition, especially under hot and dry conditions. DSS-based mild-deficit irrigation can be adopted to reduce vineyard water consumption without compromising Pinot gris wine quality.

**Keywords:** deficit irrigation; stem water potential; Pinot gris; volatile aroma compounds

Check for updates

Academic Editor: Ivan Francisco Garcia Tejero

Received: 25 May 2026
Revised: 22 June 2026
Accepted: 23 June 2026
Published: 25 June 2026



## 1. Introduction

Water availability in wine-growing regions is expected to decline in the coming years due to climate change [1], representing a major threat to global viticulture, with the potential to reduce yields and compromise wine quality [2]. Water availability is particularly crucial during early phenological stages, as water stress around flowering can reduce fruit set, while a moderate water deficit during ripening may enhance secondary metabolism [3]. Previous studies have shown that water stress can stimulate the accumulation of sugars [4], flavonoids [5], antioxidants [6], and volatile organic compounds, thereby improving grape and wine quality [7–9]. Although some studies have reported a positive effect of water deficit on the biosynthesis of aroma precursors in grapes, the impacts on wine aromatic profiles remain limited and often inconsistent [10–14].

Deficit irrigation strategies aim to maintain yield while enhancing grape quality under mild water stress conditions. These practices help optimize production and preserve water resources by minimizing transpiration during the summer months [15–18]. However, the effective implementation of deficit irrigation requires careful and continuous monitoring of vine water status. Over the past decades, several deficit irrigation strategies have been proposed, often supported by sensors and prediction models [19–22].

Pre-dawn water potential ($\Psi_{PD}$) is considered a reliable indicator of plant water status, as it directly measures the water available to the plant [23]. Although $\Psi_{PD}$ is a valuable parameter for managing irrigation [24], its measurement with a Scholander pressure chamber is time-consuming and impractical for routine application. Consequently, recent research has increasingly focused on modeling and predicting $\Psi_{PD}$ rather than relying on continuous measurements, to enable more efficient irrigation management [25,26]. In this context, the decision support system (DSS) Vintel® simulates $\Psi_{PD}$ dynamics based on meteorological and physiological parameters, allowing irrigation scheduling according to predefined thresholds aligned with enological goals.

The aim of this study was to evaluate the effects of three deficit irrigation regimes—well-watered (WW), mild deficit (MiD), and moderate deficit (MoD)—implemented through the Vintel® DSS, on vine performance, grape composition, and wine volatile profile in a Pinot gris vineyard over two contrasting seasons. This study provides new insights into how DSS-guided deficit irrigation can be applied to optimize water use while preserving vine aromatic quality under contrasting meteorological conditions.

## 2. Materials and Methods

### *2.1. Experimental Site, Plant Material, and Irrigation Treatments*

The trial was carried out at the experimental farm "A. Servadei" of the University of Udine during the 2021 and 2022 seasons. The vines were cane pruned using a single Guyot training system, with eight buds left per cane. Three adjacent rows of Pinot gris grapevines (*Vitis vinifera* L., clone R6 grafted onto SO4) were selected, and prior to the start of the experiment, three different irrigation regimes to be applied between flowering and maturation were defined based on distinct pre-dawn water potential ($\Psi_{PD}$) thresholds. The development of deficit irrigation strategies consisted of identifying suitable $\Psi_{PD}$ thresholds to serve as strategy-defining parameters in Vintel®, allowing the simulation of targeted water status levels across the phenological stages. Along each row, four plots were randomly selected. The treatments in the comparison were as follows: well-watered (WW, $\Psi_{PD} = -0.20$ MPa throughout the season); mild deficit irrigation (MiD, $\Psi_{PD} = -0.20$ MPa until flowering, $-0.35$ MPa from flowering to harvest); and moderate deficit irrigation (MoD, $\Psi_{PD} = -0.20$ MPa until flowering, $-0.55$ MPa from flowering to harvest) (Figure 1). The amount of water applied in each treatment in the two seasons is reported in Table S1.

To determine the root depth input for Vintel®, at the beginning of the experiment a pit was dug down to 1.5 m. The exposed profile showed that the larger structural roots grew down to 0.8 m, with finer roots growing deeper to 1 m; below this depth, the soil presented only gravel, and no roots were found. Based on these observations, we set the root depth to 1.0 m.

### *2.2. The Vintel® DSS*

Vintel® is a decision support system (DSS), released in 2015, developed through a collaborative project between the French company ITK and the French research institution INRAE. The purpose of Vintel® is to assist vine growers in managing vineyard operations more effectively. The irrigation module integrates several agronomic models that simulate soil and plant water status (Figure S1).

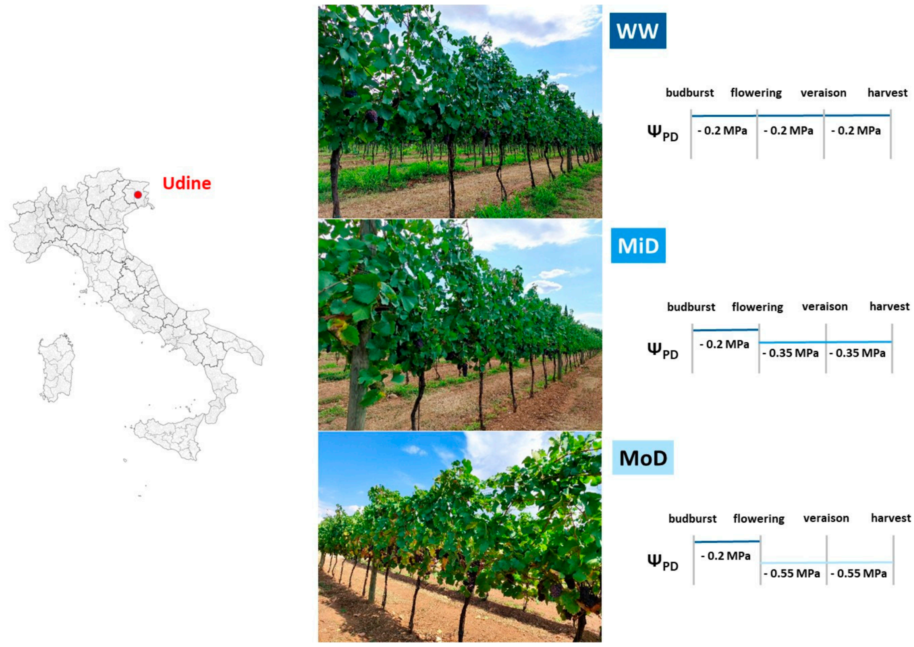


**Figure 1.** Irrigation treatments applied in a vineyard in Northeastern Italy (Udine): well-watered (WW, $\Psi_{PD} = -0.20$ MPa throughout the season—dark blue); mild deficit irrigation (MiD, $\Psi_{PD} = -0.20$ MPa until flowering, $-0.35$ MPa from flowering to harvest—medium blue), and moderate deficit irrigation (MoD, $\Psi_{PD} = -0.20$ MPa until flowering, $-0.55$ MPa from flowering to harvest—light blue).

### *2.3. Meteorological Data*

For the present experiment, data were collected from the Udine S. Osvaldo weather station, and provided by the meteorological agency of the Friuli Venezia Giulia Region (ARPA FVG–OSMER, http://www.meteo.fvg.it/, accessed on 23 January 2026). The number of tropical nights was calculated following [27], defined as the number of days when the minimum air temperature remained above 20 °C.

### *2.4. Plant Measurements, Yield, Grape Analysis and Micro-Vinification Procedure*

During both seasons, the stem water potential ($\Psi_{STEM}$) was monitored approximately every 15 days. Four fully expanded leaves from different vines were sampled in each plot. Specifically, for $\Psi_{STEM}$ measurements, leaves were bagged and enclosed in aluminum foil between 11:00 a.m. and 1:00 p.m. The leaves remained bagged for one hour to allow them and the stems to equilibrate [28]. After sampling, the leaves were detached from the vines, petioles were cut with a razor blade, and measurements were performed with a Scholander pressure chamber model 3000F01 (Soil Moisture Co., Santa Barbara, CA, USA).

From véraison to harvest, 40-berry samples were collected from each plot during both seasons, placed in plastic bags, and immediately stored in a portable fridge to preserve them until analysis. The berries were manually squeezed to determine their total soluble solids (TSS), pH, and titratable acidity (TA). TSS (°Brix) was measured using a manual refractometer model ATC-1 (Atago, Tokyo, Japan), while pH was determined using a benchtop meter model HI2211 (Hanna Instruments, Woonsocket, RI, USA). TA ($g \cdot L^{-1}$ tartaric acid equivalents) was determined by titrating the juice with 0.1 M NaOH until pH 7.

At harvest, 100-berry samples were weighed to calculate their sugar loading. Yield parameters were assessed on 10 vines per plot by weighing the harvested grapes and counting the number of clusters per vine. The average cluster weight was then calculated by dividing the yield per vine by the number of clusters.

From each plot, grapes were harvested and separately pressed using a vertical A20 pneumatic press (Grifo Marchetti, Piadena, Italy). The resulting must was transferred into 10 L glass carboys and treated with 6 g $hL^{-1}$ of $K_2S_2O_5$. Fermentation was started via the inoculation of 4 g $hL^{-1}$ of the commercial yeast strain *Saccharomyces bayanus* Mycoferm IT07 (Ever, Pramaggiore, Italy), with the temperature kept at approximately 18 °C. Sugar reduction was monitored during fermentation, and diammonium phosphate (Enologica Vason S.p.A., Verona, Italy) was added only to prevent stuck fermentation due to yeast nutrient starvation. At the end of fermentation, the wines were racked, and the carboys were transferred to 4 °C to achieve tartaric stabilization. In December, the wines were bottled and stored for subsequent chemical and sensory analysis.

Each wine was analyzed for its alcohol content (vol %) using an Alcolyzer Wine (Anton Paar Italia S.r.l., Rivoli, Italy). The malic acid concentration in the wine and yeast amino nitrogen (YAN; Table S2) in the must were quantified using a Hyperlab Plus multiparametric analyzer (Steroglass S.r.l., Perugia, Italy). The titratable acidity (TA) and pH were measured as previously described for the berry juice.

### *2.5. GC-MS Analysis of Terpenes, C13-Norisoprenoids and Fermentative Aroma Compounds in Wines*

The profiles of varietal and fermentative aroma compounds were analyzed using LLE-GC-MS and SPE-GC-MS methods, as previously reported in [29].

SPE-GC-MS was employed to quantify terpenes and $C_{13}$-norisoprenoids in free form. Extractions were performed on Isolute® C18 SPE cartridges (500 mg, 6 mL) (Biotage, Uppsala, Sweden) according to [30]. Briefly, 25 µL of internal standard (1-heptanol in 96% $v/v$ ethanol; 312 and 328 µg $mL^{-1}$ in 2021 and 2022, respectively) was added to 100 mL of wine. Cartridges were conditioned with 25 mL of methanol followed by 25 mL of Milli-Q water before sample loading. Sample loading was followed by a washing step with 150 mL of Milli-Q water, and free varietal aromas were eluted with 25 mL of pentane:dichloromethane (2:1 $v/v$). The eluate was dehydrated with anhydrous sodium sulfate and concentrated under nitrogen flow to a final volume of approximately 1 mL.

Fermentative aroma compounds were extracted from 10 mL wine samples mixed with 10 mL of 30% sodium chloride solution and 200 µL of ethyl heptanoate (Sigma-Aldrich, St. Louis, MO, USA) in 96% $v/v$ ethanol as the internal standard (0.87 and 1.17 g/L in 2021 and 2022, respectively). Extractions were performed with 5 mL of pentane/dichloromethane (2:1 $v/v$), and the glass tube was shaken vigorously by hand for 2 min; this procedure was repeated three times. The combined phases were dried over anhydrous sodium sulphate and concentrated under nitrogen flow to a final volume of approximately 1 mL.

GC-MS analysis was carried out as described for the LLE–GC–MS analysis [31], and applied to both the fermentative and varietal fractions.

Samples were analyzed using a GC-MS system consisting of a gas chromatograph (GC 7820A), an autosampler (7693A), and a quadrupole mass spectrometer (5977E MSD) (Agilent Technologies Inc., Santa Clara, CA, USA). Volatile compounds were separated on a DB-Wax capillary column (30 m × 0.25 mm i.d., 0.25 µm film thickness) (Agilent Technologies Inc., Santa Clara, CA, USA). Helium was used as the carrier gas at a constant flow rate of 1 mL $min^{-1}$. The oven temperature program was as follows: 40 °C for 5 min, followed by an increase of 4 °C per minute, up to 240 °C, which was held for 15 min. The injections were performed in splitless mode (250 °C; split vent closed for 70 s). The mass spectrometer was operated in SCAN mode (scan range $m/z$ 30–400), recording mass spectra in electron impact mode (EI) at 70 eV. The interface and source temperatures were set at 240 °C and the quadrupole temperature was set at 150 °C. Data acquisition and processing were performed using MassHunter GC-MS with MSD ChemStation DA software (Agilent Tecnologies Inc., Santa Clara, CA, USA).

https://doi.org/10.3390/agronomy16131232

Volatile compounds in the 2021 and 2022 samples were tentatively identified by comparing their mass spectra to those listed in the mass spectral libraries of the data processing software. Linear retention indices were calculated using the retention times of n-alkanes and compared with values reported in the literature. Relative quantification (expressed as internal standard equivalents) was performed by integrating the areas of the chromatographic peaks in the total ion current.

For each sample, two analytical replicates were performed.

*2.6. GC-MS/MS Analysis of Volatile Thiols*

Thiols in the wines were analyzed following the method described in [32,33]. A 50 mL wine sample was spiked with internal standards: 4-methoxy-2-methylbutane-2-thiol (4MSB, CDN Isotopes, Pointe-Claire, QC, Canada) for 4-methyl-4-sulfanyl-2-pentanone (4MSP, Merck KGaA, Darmstadt, Germany) quantification and d5 3-sulfanylhexan-1-ol (d53SH; EPTES, Vevey, Switzerland) for 3-sulfanylhexan-1-ol (3SH) and 3-sulfanylhexyl acetate (3SHA). The pH of the wine was adjusted to 5–6.

Extraction was performed on Dowex columns as described in [34]. The organic phases were evaporated under reduced pressure (250 mbar) to ~0.5 mL and transferred into 1.5 mL dark vials. Soxhlet flasks were rinsed with 0.5 mL of dichloromethane and sonicated for 1 min, and the extract was collected in 1.5 mL dark vials. Samples were concentrated under reduced pressure (100 mbar) to ~30 µL. Identification and quantification were performed using an ultra-high-sensitive gas chromatograph coupled to a triple quadrupole mass spectrometer (GCMS-TQ™8050 NX, Schimadzu, Kyoto, Japan) with an AOC-6000 autosampler, as described in [35]. A 1 µL volume of sample was injected in splitless mode at 250 °C. Separation was carried out on an HPINNOWAX column (60 m × 0.25 mm; 0.25 µm; Agilent J&W Scientific, Agilent Technologies, Santa Clara, CA, US) with helium as the carrier gas (1.0 mL $min^{-1}$). The oven temperature program was set as follows: an initial temperature of 45 °C for 1 min, increased by 5 °C $min^{-1}$ to 90 °C, then by 4 °C $min^{-1}$ to 174 °C with a 2 min hold, and finally, ramped by 20 °C $min^{-1}$ to 250 °C with a 10 min hold.

The transitions, collision energies, and validation parameters (linearity range, R, recovery, repeatability, LOD, LOQ) for the analyzed thiols are presented in [35].

Calibration was performed in 8 calibration steps in the range from 0 to 9.6 g $L^{-1}$ in synthetic wine ($R^2$ = 0.9993). The limit of detection (LOD) and limit of quantification (LOQ) were 0.1 and 0.3 ng $L^{-1}$, respectively, considering signal-to-noise ratios S/N = 3 and S/N = 10, respectively.

For each sample, two analytical replicates were performed.

*2.7. Statistical Analysis*

Data were analyzed using a two-way analysis of variance with irrigation treatment and season as factors. When the test result was significant ($p \leq 0.05$), means were compared using the pairwise Student–Newman–Keuls test ($p \leq 0.05$), considering years and irrigation treatments separately. Statistical analyses were performed with the R statistical language (version 4.2.2; R CoreTeam, Vienna, Austria).

## 3. Results

*3.1. Meteorological Trends*

In the 2021 and 2022 seasons, the meteorological conditions were markedly different, yet grapevines experienced water stress during the summer in both years (Figure 2).

In 2021, April and May were characterized by heavy rainfall, totaling 453 mm, and low temperatures, which delayed the grapevine phenology (Figure 2A). From June onward, conditions became progressively drier and warmer: average temperatures increased to

23.4 °C in June and 24.4 °C in July, with rainfall dropping to 37 mm. A single rainfall event in late July (approximately ~63 mm) coincided with véraison.

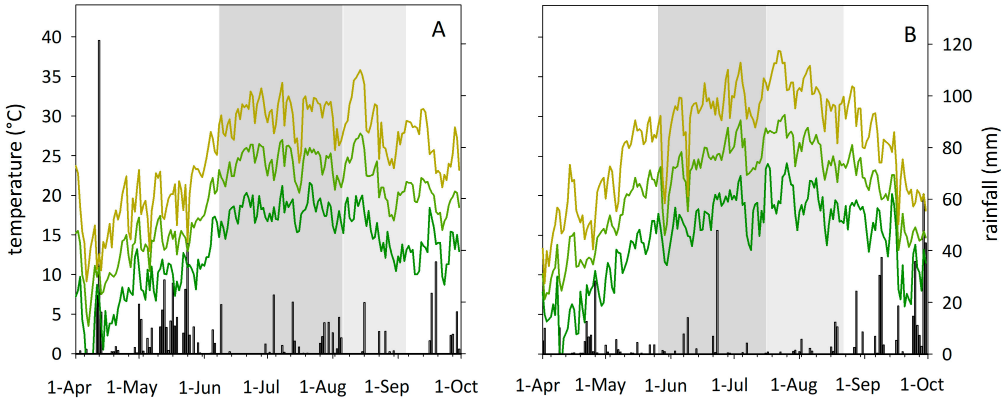


**Figure 2.** Trends of minimum (dark green), mean (medium green) and maximum temperatures (light green), and rainfall (black vertical lines) during the 2021 (**A**) and 2022 (**B**) seasons. Data were recorded at the Udine S. Osvaldo weather station (ARPA FVG–OSMER, http://www.meteo.fvg.it/ accessed on 23 January 2026). Dark gray indicates the period between flowering (EL 23) and véraison (EL 35), while pale gray indicates that between véraison and harvest (EL 38).

In August, maximum temperatures exceeded 35 °C during the first half of the month, while the mean stabilized at 22.5 °C. Rainfall was scarce and unevenly distributed, with just 40 mm recorded. Between mid-July and mid-August, six tropical nights were observed. High temperatures persisted in September, with daily maximum values above 30 °C in the first fortnight of the month, accompanied by a complete absence of rainfall.

In contrast, 2022 was warmer and drier, particularly during berry ripening (Figure 2B). After moderate rainfall in April (88 mm), precipitation declined sharply in May (28 mm) and remained limited throughout the summer. Mean temperatures reached 24.4 °C in June and 26.7 °C in July, with a maximum of 38.3 °C. The hot trend continued in August. Two significant rainfall events occurred on 18 and 28 August, accounting for 22.9 and 27 mm, respectively, but their stormy nature limited the effective replenishment of soil moisture. From mid-June to mid-August, 19 tropical nights were recorded. In September, intense storms brought over 280 mm of rainfall within the first 10 days, causing a marked drop in temperature after the harvest period. The irrigation strategies applied to the vineyard altered the total amount of water supplied during both growing seasons. In 2021, the WW treatment received 159 $m^3$ of water, whereas irrigation was reduced by 51.6% in the MiD treatment (77 $m^3$) and by 75.5% in the MoD treatment (55 $m^3$) (Table S1). In the 2022 season, the water supply was reduced by 31.1% and 39.4% in the MiD and MoD treatments, respectively, compared to WW.

### *3.2. Stem Water Potential Trends in 2021 and 2022*

Due to the contrasting meteorological conditions, both the amount of irrigated water and the trend of the measured $\Psi_{STEM}$ differed between the two seasons (Figure 3).

As expected, $\Psi_{STEM}$ values were more negative from June to August, with fluctuations influenced by the temperature, vapor pressure deficit (VPD) and rainfall distribution. In 2021, $\Psi_{STEM}$ ranged between −0.4 and −1.0 MPa on the first three sampling dates, with no significant differences among the treatments (Figure 3A). Significantly lower values were observed in MiD and MoD compared to WW only on the fourth and sixth sampling dates, while no other significant differences were detected throughout the season. In contrast, in 2022, a clearer separation among the treatments was observed throughout the summer: $\Psi_{STEM}$ values were consistently highest in WW, intermediate in MiD, and lowest in MoD, although the differences were not always statistically significant (Figure 3B). These water potential patterns confirm that the Vintel® DSS successfully maintained the intended differences in vine water status across the irrigation regimes, even under contrasting seasonal conditions.

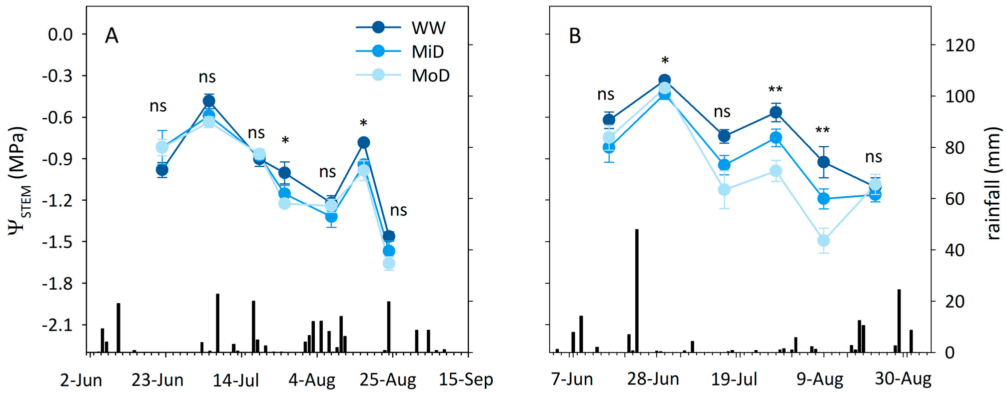


**Figure 3.** Trends of stem water potential ($\Psi_{STEM}$) during the 2021 (**A**) and 2022 (**B**) seasons for the three irrigation strategies compared. Data were analyzed through one-way ANOVA (ns, *, **: not significant and significant at $p \leq 0.05$ and $p \leq 0.01$, respectively, via F-test). Means ± SE (n = 4). WW, well-watered—dark blue; MiD, mild deficit irrigation—medium blue; MoD, moderate deficit irrigation—light blue.

This pattern reflected the prolonged absence of rainfall during that period. On the final sampling date, however, no significant differences were detected among the treatments, as rainfall had replenished the soil moisture.

### 3.3. Yield Parameters

Yield parameters were significantly affected by both treatment and season (Table 1).

**Table 1.** Effect of irrigation treatment (well-watered, WW; mild deficit irrigation, MiD; and moderate deficit irrigation, MoD) and season on yield and basic maturation parameters at harvest.

| | **Irrigation Treatment (W)** | | | | **Year (Y)** | | | **W × Y Int.** |
|---|---|---|---|---|---|---|---|---|
| | **WW** | **MiD** | **MoD** | **Sign. F** [z] | **2021** | **2022** | **Sign. F** | **Sign. F** |
| Cluster number | 25.8 ± 0.37 a [y] | 24.4 ± 0.77 ab | 23.3 ± 0.72 b | * | 27.1 ± 0.19 b | 21.9 ± 0.22 a | *** | * |
| Yield (kg vine$^{-1}$) | 3.60 ± 0.16 a | 3.08 ± 0.05 b | 2.91 ± 0.16 b | * | 2.89 ± 0.06 b | 3.50 ± 0.18 a | *** | ns |
| Cluster weight (g) | 143 ± 5.02 a | 126 ± 6.01 b | 129 ± 1.82 b | ** | 106 ± 2.19 b | 159 ± 6.25 a | *** | ns |
| Berry weight (g) | 1.32 ± 0.01 a | 1.18 ± 0.03 b | 1.04 ± 0.02 c | *** | 1.23 ± 0.00 a | 1.12 ± 0.04 b | ** | ** |
| TSS (°Brix) | 20.1 ± 0.09 a | 19.3 ± 0.22 b | 18.3 ± 0.14 c | *** | 19.2 ± 0.03 | 19.3 ± 0.23 | ns | * |
| SL (g berry$^{-1}$) | 113 ± 2.52 a | 105 ± 0.72 b | 90.0 ± 3.20 c | *** | 203 ± 0.27 a | 1.88 ± 0.08 b | * | * |
| TA (g L$^{-1}$) | 5.57 ± 0.08 | 5.19 ± 0.33 | 5.21 ± 0.29 | ns | 5.68 ± 0.19 a | 4.96 ± 0.22 b | *** | ns |
| pH | 3.43 ± 0.01 | 3.45 ± 0.02 | 3.47 ± 0.03 | ns | 3.37 ± 0.01 b | 3.53 ± 0.02 a | *** | ns |

[z] Data were analyzed through two-way ANOVA (ns, *, **, ***: not significant and significant at $p \leq 0.05$, $p \leq 0.01$, and at $p \leq 0.001$, respectively, via F-test). When the test result was significant, irrigation treatment means were separated using the Student–Newman–Keuls test ($p \leq 0.05$). Mean comparisons among the treatments are shown in Figure 4 for significant interactions. [y] Different letters identify significantly different means. Means ± SEs (n = 4). TSS, total soluble solids; SL, sugar loading; TA, titratable acidity.

Regarding irrigation, both MiD and MoD showed a significant reduction in mean cluster weight and yield compared to WW, whereas no differences were observed between MiD and MoD. Considering the seasonal factor, although the number of clusters was higher in 2021, the mean cluster weight and yield were higher in 2022, more than compensating for the lower cluster number. The deficit irrigation strategies significantly affected the number of clusters, with lower values under MoD, particularly due to the reduction observed in 2022. A significant treatment x year interaction was detected for the cluster number: in 2021, no differences emerged between the treatments, while in 2022, MoD showed a significantly lower cluster number compared to both MiD and WW (Figure 4A). The irrigation treatments also significantly influenced the berry weight, with lower values under more restricted water regimes. As for the seasonal effect, higher berry weight was recorded in 2021. A significant treatment × year interaction was also found for this parameter (Figure 4B): in 2021, a reduction in berry weight was observed only under MoD, whereas in 2022, both MiD and MoD resulted in significantly lower values compared to WW. Comparing the single treatments between the years, we found that the cluster number was significantly lower in 2022 for all treatments (Figure 4D).

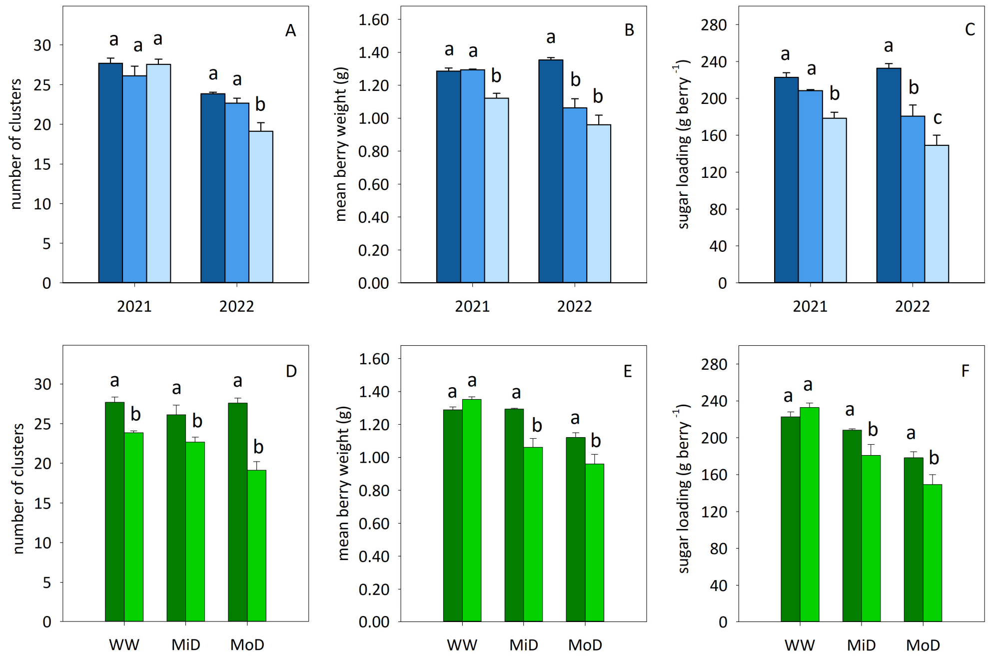


**Figure 4.** Bar plots representing the means ± SEs (n = 4) of the cluster number (**A**,**D**), berry weight (**B**,**E**), and sugar loading (**C**,**F**) in a Pinot gris vineyard under three irrigation strategies (WW, well-watered—dark blue; MiD, mild deficit irrigation—medium blue; MoD, moderate deficit irrigation—light blue), in 2021 (dark green) and 2022 (pale green) at harvest. The analysis of variance indicating a significant interaction between the irrigation strategies and year is shown in Table 1; the pairwise comparison was computed separately by year. Different letters identify significantly different means.

### 3.4. Berry Maturation Parameters

Both the irrigation treatments and the year significantly affected the total soluble solids (TSS) and an interaction between these two factors was observed (Table 1).

Samples were collected during maturation, and their basic maturation parameters were assessed (Figure 5).

TSS increased with the progression of ripening, reaching a plateau at the third sampling time. The two-way ANOVA revealed that the MiD and MoD treatments resulted in lower TSS compared to WW. More specifically, when the interaction between irrigation treatment and season was examined, significantly higher TSS values were observed for WW compared to both MiD and MoD in 2021, whereas for 2022, lower values were observed only under MoD. Consistent with TSS, sugar loading was significantly reduced under the MiD and MoD treatments, although a significant interaction between the irrigation treatments and the year was also detected (Table 1). Figure 4C shows that the MoD treatment resulted in a significantly lower value of this parameter in 2021, while in 2022, all three treatments differed significantly, with lower values recorded for MiD and, to a greater extent, MoD. The contrasting behavior of MiD across the two seasons can be explained by considering the berry weight and sugar loading (Table 1). When the single treatments were compared between the years, reduced values of the mean berry weight and sugar loading were observed for MiD and MoD, but not for WW (Figure 4E,F). The trend of titratable acidity was similar in both seasons, with no significant differences among the treatments on any sampling day or at harvest (Figure 5C,D). Conversely, significantly lower acidity was recorded in the second year of investigation. The must pH at harvest was not affected by the irrigation treatments, but a significant seasonal effect was observed, with lower values in 2021.

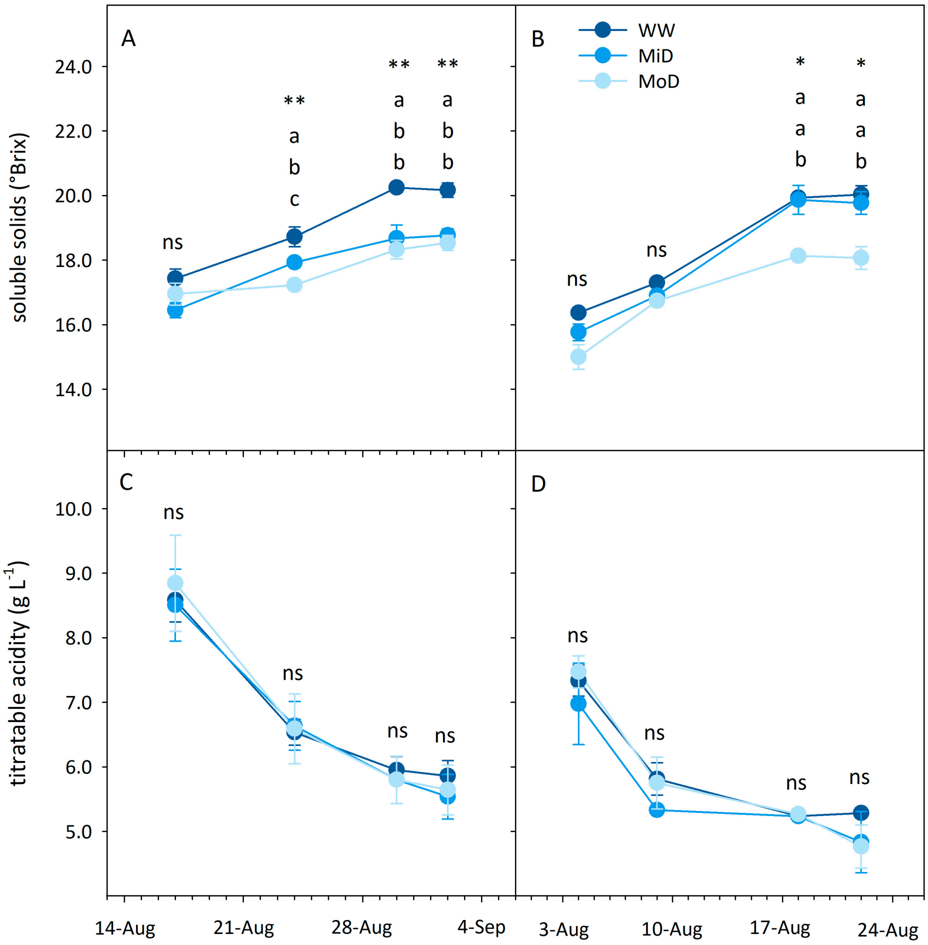


**Figure 5.** Total soluble solids (**A**,**B**) and titratable acidity (**C**,**D**) in grapes during maturation in 2021 (**A**,**C**) and 2022 (**B**,**D**). For each date, one-way ANOVA was applied (ns, *, **: not significant and significant at $p \leq 0.05$ and $p \leq 0.01$, respectively, via F-test). When the test result was significant, irrigation treatment means were separated using the Student–Newman–Keuls test ($p \leq 0.05$). Different letters identify significantly different means. Mean ± SE (n = 4). WW, well-watered; MiD, mild deficit irrigation; MoD, moderate deficit irrigation.

### 3.5. Wine Chemistry

The chemical parameters analyzed in the wines revealed significant effects of both the irrigation treatment and year (Table 2). The alcohol content was significantly affected by the irrigation treatment, with lower values under MiD and MoD. Although no main effect of season was ascertained, a significant treatment x year interaction was observed; specifically, in 2021, both MiD and MoD showed significantly lower values compared to WW, whereas in 2022, only MoD resulted in a reduction. Titratable acidity was significantly affected only by the season, with higher values in 2021—a trend consistent with that of malic acid. Regarding this acid, the irrigation treatment also showed a significant effect, with lower values observed under both MiD and MoD. Finally, although wine pH was not significantly affected by the irrigation treatment alone, a significant year x treatment interaction was detected. In 2021, pH values were generally lower, whereas in 2022, significantly lower, intermediate, and higher values were recorded under MoD, MiD, and WW, respectively.

**Table 2.** Effect of irrigation treatment and season on wine chemical parameters (well-watered, WW; mild deficit irrigation, MiD; and moderate deficit irrigation, MoD).

| | Irrigation Treatment (W) | | | | Year (Y) | | | W × Y Int. |
|---|---|---|---|---|---|---|---|---|
| | WW | MiD | MoD | Sign. F [z] | 2021 | 2022 | Sign. F | Sign. F |
| Alcohol | 12.1 ± 0.13 a [y] | 11.3 ± 0.07 b | 10.8 ± 0.16 c | *** | 11.5 ± 0.09 | 11.3 ± 0.14 | ns | * |
| TA (g $L^{-1}$) | 4.96 ± 0.09 | 4.94 ± 0.18 | 4.92 ± 0.19 | ns | 5.51 ± 0.19 a | 4.37 ± 0.12 b | *** | ns |
| Malic acid (g $L^{-1}$) | 1.19 ± 0.05 a | 0.94 ± 0.04 b | 0.94 ± 0.03 b | *** | 1.36 ± 0.05 a | 0.69 ± 0.03 b | *** | ns |
| pH | 3.27 ± 0.02 | 3.22 ± 0.04 | 3.21 ± 0.04 | ns | 3.18 ± 0.04 b | 3.29 ± 0.03 a | ** | ** |

[z] Data were analyzed through two-way ANOVA (ns, *, **, ***: not significant and significant at $p \leq 0.05$, $p \leq 0.01$ and $p \leq 0.001$, respectively, via F-test). When the test was significant, irrigation treatment means were separated using the Student–Newman–Keuls test ($p \leq 0.05$). [y] Different letters identify significantly different means. Means ± SEs (n = 4).

The wines were analyzed to assess differences in their aroma profiles due to the irrigation treatments. The identified compounds were grouped into aliphatic acids, alcohols, esters, thiols, terpenes, $C_{13}$-norisoprenoids, and others.

Nine aliphatic acids were detected, with acetic, octanoic, and hexanoic acids showing the highest concentrations (Table 3). The total concentration of aliphatic acids was not significantly affected by deficit irrigation. However, MoD wines showed significantly lower concentrations of 2-methylpropropanoic acid and 2-methylbutanoic acid, while MiD wines had higher levels of decanoic acid. By contrast, all aliphatic acids were significantly affected by the season. Although the differences were not statistical, the total aliphatic acid concentration tended to be higher in WW and MiD wines. Most compounds showed slightly higher concentrations in MiD compared to WW. Conversely, shorter-chain aliphatic acids were slightly reduced in MoD wines.

Higher alcohols were the second major class of aroma compounds detected in the Pinot gris wines. Within this group, the highest concentrations were measured for 3-methyl-1-butanol, phenylethyl alcohol, and 2-methyl-1-propanol (Table 3). As with the aliphatic acids, their concentration was not significantly affected by deficit irrigation, but instead showed a strong seasonal effect, with higher levels in 2022. Among the higher alcohols, only phenylethyl alcohol was significantly influenced by irrigation, with higher values under WW and lower values under MiD. Although no significant effects were observed for the other alcohols, a trend emerged: total concentrations were slightly higher under WW and lower under the other treatments. While 2-methyl-1-propanol, 1-butanol and 3-methyl-1-butanol were scarcely affected by the irrigation treatments, more evident differences appeared for the remaining compounds, with slightly lower values under MoD.

Eleven esters were identified in the aromatic profile of the Pinot gris wines. The highest concentrations were found for ethyl octanoate and 3-methylbutyl acetate (Table 3). The irrigation treatments did not significantly affect either the total ester concentration or individual compounds, except for diethyl 2-hydroxybutanedioate, which showed higher levels under WW. In contrast, the season strongly impacted seven esters, with higher concentrations in 2022. Although the irrigation treatments had only minor effects, a trend was observed toward slightly higher concentrations under WW, while MiD and MoD showed similarly lower values.

Among the other compounds, 3-hydroxybutan-2-one was the only aroma compound significantly affected by the irrigation regime, showing lower concentrations under WW and MiD and higher levels under MoD. The other two compounds were unaffected by irrigation but, together with 3-hydroxybutan-2-one, were instead affected by the season, with higher values in 2022 (Table 3).

**Table 3.** Effect of irrigation level and season on wine aroma compounds μg $L^{-1}$ (except for thiols, which are reported in ng $L^{-1}$). WW, well-watered; MiD, mild deficit irrigation; MoD, moderate deficit irrigation.

| | | Irrigation Treatment (W) | | | | Year (Y) | | | |
|---|---|---|---|---|---|---|---|---|---|
| **Aromatic Group** | **Aroma Compound** | **WW** | **MiD** | **MoD** | **Sign. F** [z] | **2021** | **2022** | **Sign. F** | **Sign. F** |
| aliphatic acids | acetic acid | 5426 ± 1262 | 4525 ± 451 | 3505 ± 481 | ns | 1413 ± 522 b [y] | 7558 ± 552 a | *** | ns |
| | propanoic acid | 137 ± 17.1 | 145 ± 22.3 | 118 ± 3.13 | ns | 35.0 ± 0.49 a | 231 ± 23.1 b | *** | ns |
| | 2-methylpropanoic acid | 446 ± 42.5 a | 431 ± 25.1 a | 318 ± 14.7 b | * | 241 ± 17.9 b | 556 ± 23.6 a | *** | ns |
| | butanoic acid | 248 ± 32.0 | 290 ± 16.1 | 254 ± 25.2 | ns | 172 ± 22.8 b | 356 ± 4.48 a | *** | ns |
| | 2-methylbutanoic acid | 463 ± 92.2 a | 396 ± 8.41 ab | 261 ± 15.3 b | ** | 271 ± 35.2 b | 476 ± 36.0 a | *** | ns |
| | hexanoic acid | 1385 ± 107 | 1656 ± 76.4 | 1646 ± 172 | ns | 1187 ± 67.5 b | 1938 ± 70.0 a | *** | * |
| | heptanoic acid | 145 ± 6.53 | 182 ± 31.3 | 145 ± 8.98 | ns | 62.0 ± 7.10 b | 253 ± 5.18 a | *** | ns |
| | octanoic acid | 2659 ± 193 | 2970 ± 154 | 3079 ± 335 | ns | 2463 ± 123 b | 3343 ± 80.3 a | *** | *** |
| | decanoic acid | 713 ± 77.4 b | 1105 ± 129 a | 721 ± 104 b | ** | 448 ± 32.8 b | 1245 ± 80.4 a | *** | *** |
| alcohols | 2-methyl-1-propanol | 10,873 ± 1200 | 9817 ± 797 | 10,392 ± 1014 | ns | 6337 ± 669 b | 14,384 ± 468 a | *** | ns |
| | 1-butanol | 247 ± 22.2 | 253 ± 24.8 | 251 ± 13.6 | ns | 142 ± 2.25 b | 358 ± 21.9 a | *** | ns |
| | 3-methyl-1-butanol | 112,241 ± 11,525 | 106,719 ± 7124 | 109,310 ± 6161 | ns | 96,092 ± 5450 b | 122,755 ± 1952 a | * | ns |
| | 1-hexanol | 593 ± 52.4 | 668 ± 45.4 | 545 ± 64.8 | ns | 412 ± 12.3 b | 793 ± 46.2 a | *** | ns |
| | 4-methyl-1-pentanol | 24.4 ± 4.28 | 22.9 ± 1.40 | 20.1 ± 3.04 | ns | 18.2 ± 5.19 b | 26.8 ± 0.57 a | * | ns |
| | 3-ethoxy-1-propanol | 772 ± 278 | 442 ± 25.1 | 491 ± 69.0 | ns | 639 ± 198 | 497 ± 56.8 | ns | ns |
| | (R,R)-2,3-Butanediol | 6722 ± 1327 | 6305 ± 593 | 4854 ± 530 | ns | 880 ± 119 b | 11,040 ± 1378 a | *** | ns |
| | (R,S)-2,3-Butanediol | 1500 ± 242 | 1595 ± 232 | 1171 ± 235 | ns | 315 ± 35.0 b | 2529 ± 359 a | *** | ns |
| | methionol | 419 ± 57.4 | 411 ± 47.2 | 351 ± 29.0 | ns | 204 ± 9.29 b | 584 ± 51.6 a | *** | ns |
| | 2-phenylethanol | 26,250 ± 1316 a | 20,321 ± 858 b | 22,282 ± 860 ab | ** | 16,342 ± 731 b | 29,560 ± 1149 a | *** | ns |
| esters | 3-methylbutyl acetate | 810 ± 157 | 625 ± 28.8 | 902 ± 133 | ns | 1097 ± 140 a | 460 ± 41.2 b | *** | * |
| | ethyl hexanoate | 493 ± 34.6 | 571 ± 41.8 | 586 ± 51.4 | ns | 402 ± 38.1 b | 698 ± 38.1 a | *** | ns |
| | ethyl 2-oxopropanoate | 242 ± 42.1 | 209 ± 22.5 | 178 ± 42.7 | ns | 230 ± 49.3 | 189 ± 13.9 | ns | ns |
| | ethyl 2-hydroxypropanoate | 2070 ± 114 | 1807 ± 164 | 1863 ± 98.3 | ns | 1657 ± 147 b | 2170 ± 118 a | ** | * |
| | ethyl octanoate | 1402 ± 553 | 663 ± 119 | 653 ± 52.7 | ns | 1257 ± 357 | 555 ± 20.5 | ns | ns |
| | ethyl 3-hydroxybutanoate | 104 ± 6.24 | 120 ± 3.62 | 104 ± 12.0 | ns | 75.3 ± 12.2 b | 143 ± 3.62 a | *** | ns |
| | ethyl decanoate | 318 ± 55.4 | 228 ± 17.8 | 249 ± 45.3 | ns | 284 ± 22.1 | 247 ± 18.3 | ns | ns |
| | phenethyl acetate | 69.6 ± 3.62 | 72.6 ± 1.98 | 80.5 ± 8.90 | ns | 60.5 ± 4.02 b | 88 ± 2.47 a | ** | *** |
| | diethyl succinate | 564 ± 38.9 | 651 ± 91.9 | 643 ± 59.1 | ns | 142 ± 12.5 b | 1097 ± 78.7 a | *** | ns |
| | diethyl malate | 262 ± 17.8 a | 175 ± 21.3 b | 176 ± 21.4 b | ** | 97.2 ± 8.81 b | 311 ± 16.5 a | *** | ns |
| | ethyl hydrogen succinate | 2175 ± 172 | 2785 ± 386 | 2234 ± 148 | ns | 364 ± 33.2 b | 4433 ± 160 a | *** | ns |
| terpenes | linalool | 1.46 ± 0.11 a | 1.07 ± 0.11 b | 1.10 ± 0.04 b | * | 1.50 ± 0.03 a | 0.91 ± 0.02 b | *** | ns |
| | β-citronellol | 10.5 ± 4.30 | 10.2 ± 2.58 | 13.0 ± 0.26 | ns | 12.7 ± 3.47 | 9.78 ± 1.10 | ns | ns |
| | geraniol | 7.00 ± 1.42 | 5.50 ± 1.10 | 4.26 ± 0.97 | ns | 4.49 ± 1.78 | 6.68 ± 0.67 | ns | ns |
| | nerolidol | 9.24 ± 3.45 | 8.87 ± 1.80 | 4.12 ± 0.19 | ns | 5.65 ± 1.22 | 9.17 ± 0.26 | ns | ns |
| | farnesol | 14.7 ± 2.42 | 12.7 ± 1.04 | 11.3 ± 2.53 | ns | 12.7 ± 2.60 | 13.1 ± 1.11 | ns | ns |
| $C_{13}$-norisoprenoids | β-damascenone | 8.17 ± 0.58 | 8.36 ± 0.60 | 9.48 ± 0.11 | ns | 12.4 ± 0.60 a | 4.93 ± 0.07 b | *** | ** |
| | 3-oxo-α-ionol | 0.82 ± 0.09 | 2.56 ± 1.11 | 1.05 ± 0.04 | ns | 0.96 ± 0.68 | 1.99 ± 0.10 | ns | ns |
| thiols | 3SHA (3-mercaptohexyl acetate) | 5.26 ± 0.10 | 4.88 ± 0.12 | 4.76 ± 0.31 | ns | 3.15 ± 0.16 b | 6.79 ± 0.31 a | *** | * |
| | 3SH (3-mercaptohexan-1-ol) | 660 ± 24.3 | 655 ± 26.7 | 602 ± 15.1 | ns | 704 ± 14.2 a | 573 ± 14.5 b | *** | ns |
| | phenylmethanethiol | 5.26 ± 0.10 | 4.88 ± 0.12 | 4.76 ± 0.31 | ns | 3.15 ± 0.16 b | 6.79 ± 0.31 a | *** | * |
| others | 3-hydroxy-2-butanone | 1277 ± 350 b | 2295 ± 391 b | 3791 ± 267 a | ** | 1633 ± 195 b | 3275 ± 549 a | ** | ns |
| | oxolan-2-one | 432 ± 32.8 | 391 ± 38.6 | 372 ± 12.6 | ns | 178 ± 11.8 b | 618 ± 45.3 a | *** | ns |
| | ethyl 5-oxotetrahydro-2-furancarboxylate | 349 ± 9.84 | 375 ± 26.4 | 354 ± 24.8 | ns | 90.9 ± 2.42 b | 628 ± 22.5 a | *** | ns |
| | total aliphatic acids | 11,622 ± 1678 | 11,701 ± 821 | 10,046 ± 1051 | ns | 6290 ± 663 b | 15,955 ± 681 a | *** | ns |
| | total higher alcohols | 159,642 ± 14,818 | 146,554 ± 6668 | 149,666 ± 8830 | ns | 121,380 ± 6799 b | 182,528 ± 4997 a | *** | ns |
| | total esters | 8510 ± 977 | 7907 ± 359 | 7668 ± 409 | ns | 5666 ± 655 b | 10,391 ± 127 a | *** | ns |
| | total terpenes | 42.9 ± 7.51 | 38.3 ± 5.31 | 33.7 ± 3.44 | ns | 37.0 ± 7.25 | 39.7 ± 3.02 | ns | ns |
| | total $C_{13}$-norisoprenoids | 8.99 ± 0.56 | 10.9 ± 1.11 | 10.5 ± 0.15 | ns | 13.4 ± 1.08 a | 6.93 ± 0.14 b | *** | * |
| | total thiols | 665 ± 24.2 | 660 ± 26.8 | 607 ± 14.9 | ns | 708 ± 14.4 a | 580 ± 14.8 b | *** | ns |

[z] Data were analyzed through two-way ANOVA (ns, *, **, ***: not significant and significant at $p \leq 0.05$, $p \leq 0.01$ and at $p \leq 0.001$, respectively, via F-test). When the test result was significant, irrigation treatment means were separated using the Student–Newman–Keuls test ($p \leq 0.05$). [y] Different letters identify significantly different means. Means ± SEs (n = 4).

Regarding terpenes, five compounds were identified across the two seasons, with β-citronellol and farnesol showing the highest concentrations (Table 3). The irrigation treatments did not significantly affect the total terpene levels or most individual compounds, except for neroditol, which was higher under WW. Although not significant, a clear trend was observed for the other terpenes, with slightly higher values under WW and lower values under MiD and MoD, especially under the latter. Seasonal effects were weaker for terpenes compared to those of the other aroma groups, with only linalool showing a significant decrease in 2022.

For $C_{13}$-norisoprenoids, only two compounds were detected, with β-damascenone being the most abundant (Table 3). The irrigation treatment had no significant effect, though slightly higher values were observed under MiD and MoD. In contrast, their concentrations were significantly higher in 2021. Finally, volatile thiols were only marginally affected by the irrigation regime, with slightly higher values under WW, whereas the season had a significant impact, with higher concentrations in 2022 (Table 3).

## 4. Discussion

In the context of climate change, irrigation strategies that reduce water use while maintaining yield and quality are increasingly important for the viticultural sector. A key objective of decision support systems (DSSs) is, therefore, to optimize water use in vineyards. In this study, we employed a DSS predicting the pre-dawn water potential ($\Psi_{PD}$) to manage three deficit irrigation strategies (well-watered, WW; mild deficit irrigation, MiD; and moderate deficit irrigation, MoD) in an experimental vineyard, thereby reducing the water supplied in the two water regimes, MiD and MoD, compared to WW.

Both deficit irrigation treatments reduced the yield, primarily through a decrease in cluster weight, while in 2022, a significantly lower cluster number was observed under MoD. Previous studies have demonstrated that water stress reduces mean cluster weight [5,8]. In addition, several authors have reported that water stress in one season may impair bud fertility and the number of berries per bunch, consequently reducing both cluster weight and number in the following year [35,36].

The contrasting meteorological conditions of the two seasons affected both total soluble solids accumulation and berry water content. Drought is known to limit sugar accumulation in grape berries, although this effect is often masked by berry dehydration, which concentrates solutes [37]. Sugar loading, which reflects the absolute amount of sugars accumulated regardless of berry size or dilution, showed a clear trend of reduction under increasing water stress, as previously reported by Wang et al. [38]. Although $\Psi_{STEM}$ values were more negative in July and August, water stress remained moderate, allowing greater water accumulation in MiD berries and leading to lower TSS. Reduced sugar loading due to photosynthetic limitation was evident mainly under MoD and, in 2022, also under MiD [16,39]. The titratable acidity and pH were only marginally affected by the irrigation treatment, while seasonal conditions had a stronger influence. The effect of temperature on titratable acidity is well known and mainly linked to malic acid respiration [40–42]. As noted above, the higher temperatures in 2022 explained the lower titratable acidity observed in the grape berries. The deficit irrigation strategies also influenced wine quality. In both seasons, the basic physico-chemical parameters of the wines (alcohol content, titratable acidity, malic acid, and pH) reflected the trends observed in the grape composition at maturity.

Beyond the physiological and compositional responses, it is worth noting the functional performance of the DSS employed to apply the targeted irrigation regimes. Rather than assessing the accuracy of punctual $\Psi_{PD}$ predictions, the focus of its application was on its capacity to maintain vines within defined water deficit ranges over time. The DSS effectively guided irrigation decisions under contrasting seasonal conditions, ensuring consistent control of vine water status and enabling reproducible stress management. This demonstrates its practical value as a tool for implementing deficit irrigation strategies in commercial viticulture.

Irrigation strategies can also affect the biosynthesis of free and bound aroma compounds, with the outcome depending on the timing and intensity of the water deficit [8]. In this study, we focused on free aroma compounds in the wines, as the aim was to assess the direct impact of deficit irrigation on the final wine quality. Seasonal variation exerted a greater influence on aroma compounds than the irrigation treatments, whereas the effect of the water regimes was comparatively limited. This finding is not surprising, as seasonal conditions are known to be a primary determinant of grapevine and wine quality. Regarding water availability, seasonal variability can have a greater effect on vineyard water status than the differences imposed by the irrigation treatments. Moreover, the seasonal factor contains multiple explanatory variables, including phenological development and climatic conditions, whereas the irrigation regime accounts solely for the amount of water supplied. Consequently, this broader range of environmental factors is likely responsible for the season's stronger impact on the aroma profile. Given the inconsistent effects of the irrigation strategies across the different classes of compounds, the results were examined by compound class.

Most aliphatic acids were marginally affected by the irrigation strategies, although they showed strong seasonal variability. Information on these compounds in the literature remains limited. In wines, Lizama et al. [13] found that under non-irrigated conditions, cv. Bobal presents an increased concentration of 2-methylpropropanoic acid, a result that contrasts with our findings. Overall, the impact of water stress on aliphatic acids in wines remains poorly understood, making it difficult to assess the fate of these compounds.

In the Pinot gris wines from this experiment, deficit irrigation led to a slight reduction in higher alcohols. Consistent with Zhu et al. [14], although not statistically significant, slightly lower concentrations of 3-methyl-1-butanol were observed under both deficit irrigation treatments. In contrast, Talaverano et al. [12], Lizama et al. [13], and Zhu et al. [14] reported an increase in most higher alcohols under deficit irrigation.

Among the aroma compounds, esters represent a key group, as they largely contribute to positive sensory attributes in wines. In our study, ester concentrations were slightly lower in 2021, whereas higher values were observed in the warmer 2022 season, regardless of the irrigation regime. The irrigation treatment did not significantly affect ester concentrations, although MiD and MoD showed slightly reduced levels. Literature results on the effect of vine water status on ester composition are inconsistent, as already reported for other aroma compounds. Diverres et al. [43] reported higher ester concentrations under heavier irrigation, while Qian et al. [10] observed an increase under deficit irrigation. Ou et al. [11] found no significant irrigation effects along with variable seasonal trends. Similarly, Zhu et al. [14] reported that water deficit altered the ester profile, with some compounds increasing and others decreasing.

Slightly lower terpene concentrations were observed in MiD and MoD Pinot gris wines. Among the individual compounds, only linalool was significantly reduced under deficit irrigation, whereas β-citronellol was higher in MoD, consistent with Zhu et al. [14]. Both the MiD and MoD treatments showed lower TSS than WW, suggesting that the water deficit delayed grape maturation. Previous studies have reported that free monoterpene concentrations in wines increase with higher berry sugar levels [44]. In line with these studies, linalool decreased together with berry sugars under water deficit in our experiment. Conversely, excessive sunlight exposure can impair aroma biosynthesis [45]. In our experiment, cluster exposure was greater in MoD due to basal leaf shedding occurring from véraison to harvest in both seasons.

For $C_{13}$-norisoprenoids, no differences were detected among the irrigation treatments, although MiD and MoD showed a trend toward higher concentrations. It is well known that water stress increases the concentration of $C_{13}$-norisoprenoids by enhancing the biosynthesis of their precursors, a process also stimulated by greater berry sunlight exposure [46,47].

Thiols were minimally affected by the irrigation treatments, showing strong seasonal variation. Moderate water stress appears to favor the biosynthesis of thiol precursors and their subsequent release in wine, whereas moderate-to-severe stress is detrimental [48], as also observed in the present study.

Water stress is also responsible for higher sunlight exposure of grape berries. Berry temperature is known to affect not only sugar accumulation, but also the biosynthesis of aroma compounds, although the reported effects are sometimes inconsistent in the literature. Palai et al. [8] demonstrated that the biosynthesis of most aroma compounds is enhanced when water stress is applied before véraison, suggesting that an increase in cluster temperature at early maturation stages can enhance the aromatic potential of the berries.

Overall, the results indicate that the DSS-based deficit irrigation strategies successfully reduced water use while maintaining a controlled vine water status under contrasting seasonal conditions. Although moderate and more severe deficit irrigation reduced the yield and slightly altered the grape composition, its effects on wine aroma were generally limited compared with the strong influence of seasonal climatic variability. These findings support the use of DSS-guided deficit irrigation as a practical approach to improve water-use efficiency in vineyards while preserving the main quality attributes of Pinot gris wines.

## 5. Conclusions

Although most effects were not statistically significant, our results suggest that moderate-to-severe water stress may negatively affect the aromatic profile of Pinot gris wines in Friuli Venezia Giulia. To preserve an optimal aroma composition, moderate-to-severe water stress (MoD) should therefore be avoided.

This study demonstrated that deficit irrigation strategies based on the pre-dawn water potential can be successfully implemented in Pinot gris vineyards using the Vintel® DSS. Mild deficit irrigation maintained the wine composition with minimal modifications of the volatile aroma profile, while moderate deficit reduced sugar accumulation and negatively affected several aromatic compounds. Overall, these results indicate that DSS-guided mild deficit irrigation can be adopted to reduce water consumption in cool-climate viticulture without compromising Pinot gris wine quality.

**Supplementary Materials:** The following supporting information can be downloaded at: https://www.mdpi.com/article/10.3390/agronomy16131232/s1. Figure S1: The algorithm used in the Vintel® DSS to calculate the amount of water to be applied in the vineyard. To run the models, inputs such as local meteorological conditions, soil characteristics, and vineyard practices must be provided. Weather data can be obtained either from physical weather stations or from a weather data provider MAXAR via ITK. Vintel® operates on a daily simulation time step, modeling $\Psi_{PD}$ in real time and providing irrigation recommendations to users. $\Psi_{PD}$ serves as a key indicator of the vine's water status and is used to calculate vine water requirements according to a predefined plant water dynamic, tailored to the desired wine profile. To model $\Psi_{PD}$, Vintel® employs the Fraction of Transpirable Soil Water (FTSW), as described by Lebon et al. [49] and by Pellegrino et al. [50]. The FTSW is calculated daily by first estimating the Total Transpirable Soil Water (TTSW) from soil characteristics, then computing the Transpirable Soil Water (TSW) through a simple water balance equation. Inputs include precipitation, irrigation, and upward water fluxes from lower soil layers, while losses account for evaporation, transpiration, and downward water fluxes. Transpiration is estimated using the Penman—Monteith model (FAO approach) and based on principles outlined by Feddes et al. [51]. Intercepted radiation is quantified according to the model from Riou et al. [52], which incorporates canopy geometry. The amount of water lost through transpiration is directly related to the transpirable soil water, as described by Lebon et al. [49]. The wet bulb model is applied to calculate the maximum volume of water that can be supplied through irrigation, based on the emitter spacing, geometry, and root volume [53]. Furthermore, Vintel® accounts for cover crops and their competition for water by dynamically modeling their daily transpiration according to the species, canopy cover, and growth stage. Table S1: Irrigation volumes applied in the WW, MD and SD treatments in the 2021 and 2022 seasons. Table S2: Initial concentrations of yeast amino nitrogen (YAN) in the must before the beginning of fermentation in the 2021 and 2022 seasons. Table S3: Volatile compounds analyzed in the wines, retention indices, standards used in identification, identification methods, and literature references.

**Author Contributions:** P.S.: Conceptualization, Investigation, Data curation, Writing—original draft, Writing—review and editing, Supervision, Funding acquisition. M.S.: Writing—original draft, Data curation, Formal analysis. A.P.: Investigation, Writing—review and editing. L.T.: Investigation, Writing—review and editing. P.C.: Writing—review and editing. A.C.: Investigation, Data curation, Writing—original draft, Writing—review and editing. S.T.: Writing—review and editing. K.L.: Investigation, Data curation, Writing—review and editing, Funding acquisition. A.V.: Investigation, Data curation, Writing—review and editing. All authors have read and agreed to the published version of the manuscript.

**Funding:** This research was funded through for the financial support provided by the "Acquavitis" project, which was implemented as part of the 2014−2020 V-A Italy Slovenia−Interreg Program, and by the "Irrigavit" project, which was implemented as part of the 2021–2027 VI-A Italy Slovenia−Interreg Program, funded by the European Regional Development Fund. This work was supported by the Complementary Operational Program of the Autonomous Region of Friuli Venezia Giulia 2014–2020 (CUP G23C25000880002—Operation Code 2025/13846—Project Code 2025/13846/14).

**Data Availability Statement:** Data will be made available on request to the authors.

**Acknowledgments:** We thank Gianni Tassan and Moreno Greatti from the University of Udine's experimental farm "A. Servadei" for their help during the set up and the conduction of the experiments. Moreover, we would like to thank Giulia Birarda, Paolo Bomben, Riccardo Braidotti, Alberto Calderan, and Tommaso Terrosi for their help during field measurements, microvinifications, and laboratory analysis. During the preparation of this work, the authors used ChatGPT (GPT-5.5) in order to improve the readability of the text. After using this tool/service, the authors reviewed and edited the content as needed and take full responsibility for the content of the published article.

**Conflicts of Interest:** Author Amelia Caffarra was employed by the company ITK. The remaining authors declare that the research was conducted in the absence of any commercial or financial relationships that could be construed as a potential conflict of interest.

## References

1. Mariotti, A.; Pan, Y.; Zeng, N.; Alessandri, A. Long-Term Climate Change in the Mediterranean Region in the Midst of Decadal Variability. *Clim. Dyn.* **2015**, *44*, 1437–1456. [CrossRef]
2. Sodini, M.; Callesen, T.; Canton, M.; Tezza, L.; Bastos Campos, F.; Zanotelli, D.; Tarolli, P.; Sivilotti, P.; Pitacco, A.; Tagliavini, M. Major Threats Caused by Climate Change to Grapevine. *Italus Hortus* **2023**, *30*, 1–24. [CrossRef]
3. Yang, C.; Menz, C.; Fraga, H.; Costafreda-Aumedes, S.; Leolini, L.; Ramos, M.C.; Molitor, D.; Van Leeuwen, C.; Santos, J.A. Assessing the Grapevine Crop Water Stress Indicator over the Flowering-Veraison Phase and the Potential Yield Lose Rate in Important European Wine Regions. *Agric. Water Manag.* **2022**, *261*, 107349. [CrossRef]
4. Canoura, C.; Kelly, M.T.; Ojeda, H. Effect of Irrigation and Timing and Type of Nitrogen Application on the Biochemical Composition of *Vitis vinifera* L. Cv. Chardonnay and Syrah Grapeberries. *Food Chem.* **2018**, *241*, 171–181. [CrossRef] [PubMed]

5. Sivilotti, P.; Calderan, A.; Braidotti, R.; Filippi, A.; Vuerich, M.; Petrussa, E.; Cogato, A.; Bavčar, D.; Lisjak, K.; Vanzo, A. Anthocyanin and Proanthocyanidin Evolution during Ripening of the Refošk Grapevine Is Modulated by Deficit Irrigation. *VITIS-J. Grapevine Res.* **2024**, *63*, 12. [CrossRef]
6. Salazar-Parra, C.; Aguirreolea, J.; Sánchez-Díaz, M.; Irigoyen, J.J.; Morales, F. Climate Change (Elevated $CO_2$, Elevated Temperature and Moderate Drought) Triggers the Antioxidant Enzymes' Response of Grapevine Cv. Tempranillo, Avoiding Oxidative Damage. *Physiol. Plant.* **2012**, *144*, 99–110. [CrossRef] [PubMed]
7. Savoi, S.; Wong, D.C.J.; Arapitsas, P.; Miculan, M.; Bucchetti, B.; Peterlunger, E.; Fait, A.; Mattivi, F.; Castellarin, S.D. Transcriptome and Metabolite Profiling Reveals That Prolonged Drought Modulates the Phenylpropanoid and Terpenoid Pathway in White Grapes (*Vitis vinifera* L.). *BMC Plant Biol.* **2016**, *16*, 67. [CrossRef] [PubMed]
8. Palai, G.; Caruso, G.; Gucci, R.; D'Onofrio, C. Water Deficit before Veraison Is Crucial in Regulating Berry VOCs Concentration in Sangiovese Grapevines. *Front. Plant Sci.* **2023**, *14*, 1117572. [CrossRef] [PubMed]
9. Bonada, M.; Jeffery, D.W.; Petrie, P.R.; Moran, M.A.; Sadras, V.O. Impact of Elevated Temperature and Water Deficit on the Chemical and Sensory Profiles of Barossa Shiraz Grapes and Wines: Temperature and Water Effects on Grapes and Wines. *Aust. J. Grape Wine Res.* **2015**, *21*, 240–253. [CrossRef]
10. Qian, M.C.; Fang, Y.; Shellie, K. Volatile Composition of Merlot Wine from Different Vine Water Status. *J. Agric. Food Chem.* **2009**, *57*, 7459–7463. [CrossRef] [PubMed]
11. Ou, C.; Du, X.; Shellie, K.; Ross, C.; Qian, M.C. Volatile Compounds and Sensory Attributes of Wine from Cv. Merlot (*Vitis vinifera* L.) Grown under Differential Levels of Water Deficit with or without a Kaolin-Based, Foliar Reflectant Particle Film. *J. Agric. Food Chem.* **2010**, *58*, 12890–12898. [CrossRef] [PubMed]
12. Talaverano, I.; Valdés, E.; Moreno, D.; Gamero, E.; Mancha, L.; Vilanova, M. The Combined Effect of Water Status and Crop Level on Tempranillo Wine Volatiles. *J. Sci. Food Agric.* **2017**, *97*, 1533–1542. [CrossRef] [PubMed]
13. Lizama, V.; Pérez-Álvarez, E.P.; Intrigliolo, D.S.; Chirivella, C.; Álvarez, I.; García-Esparza, M.J. Effects of the Irrigation Regimes on Grapevine Cv. Bobal in a Mediterranean Climate: II. Wine, Skins, Seeds, and Grape Aromatic Composition. *Agric. Water Manag.* **2021**, *256*, 107078. [CrossRef]
14. Zhu, Y.; Sun, M.; Harrison, R.; Jordan, B.; Creasy, G.; Hofmann, R. Effects of UV-B and Water Deficit on Aroma Precursors in Grapes and Flavor Release during Wine Micro-Vinification and Consumption. *Foods* **2022**, *11*, 1336. [CrossRef] [PubMed]
15. Costa, J.M.; Ortuño, M.F.; Chaves, M.M. Deficit Irrigation as a Strategy to Save Water: Physiology and Potential Application to Horticulture. *J. Integr. Plant Biol.* **2007**, *49*, 1421–1434. [CrossRef]
16. Chaves, M.M.; Zarrouk, O.; Francisco, R.; Costa, J.M.; Santos, T.; Regalado, A.P.; Rodrigues, M.L.; Lopes, C.M. Grapevine under Deficit Irrigation: Hints from Physiological and Molecular Data. *Ann. Bot.* **2010**, *105*, 661–676. [CrossRef] [PubMed]
17. Permanhani, M.; Costa, J.M.; Conceição, M.A.F.; De Souza, R.T.; Vasconcellos, M.A.S.; Chaves, M.M. Deficit Irrigation in Table Grape: Eco-Physiological Basis and Potential Use to Save Water and Improve Quality. *Theor. Exp. Plant Physiol.* **2016**, *28*, 85–108. [CrossRef]
18. Cabral, I.L.; Teixeira, A.; Lanoue, A.; Unlubayir, M.; Munsch, T.; Valente, J.; Alves, F.; Da Costa, P.L.; Rogerson, F.S.; Carvalho, S.M.P.; et al. Impact of Deficit Irrigation on Grapevine Cv. 'Touriga Nacional' during Three Seasons in Douro Region: An Agronomical and Metabolomics Approach. *Plants* **2022**, *11*, 732. [CrossRef] [PubMed]
19. Intrigliolo, D.S.; Pérez, D.; Risco, D.; Yeves, A.; Castel, J.R. Yield Components and Grape Composition Responses to Seasonal Water Deficits in Tempranillo Grapevines. *Irrig. Sci.* **2012**, *30*, 339–349. [CrossRef]
20. Deloire, A.; Pellegrino, A.; Rogiers, S. A Few Words on Grapevine Leaf Water Potential. *Tech. Rev.* **2020**, *20*. [CrossRef]
21. Duan, B.; Mei, Y.; Chen, G.; Su-Zhou, C.; Li, Y.; Merkeryan, H.; Cui, P.; Liu, W.; Liu, X. Deficit Irrigation and Leaf Removal Modulate Anthocyanin and Proanthocyanidin Repartitioning of Cabernet Sauvigno (*Vitis vinifera* L.) Grape and Resulting Wine Profile. *J. Sci. Food Agric.* **2022**, *102*, 2937–2949. [CrossRef] [PubMed]
22. Romero, P.; Pérez-Pérez, J.G.; Del Amor, F.M.; Martinez-Cutillas, A.; Dodd, I.C.; Botía, P. Partial Root Zone Drying Exerts Different Physiological Responses on Field-Grown Grapevine (*Vitis vinifera* Cv. Monastrell) in Comparison to Regulated Deficit Irrigation. *Funct. Plant Biol.* **2014**, *41*, 1087. [CrossRef] [PubMed]
23. Tomasella, M.; Calderan, A.; Mihelčič, A.; Petruzzellis, F.; Braidotti, R.; Natale, S.; Lisjak, K.; Sivilotti, P.; Nardini, A. Best Procedures for Leaf and Stem Water Potential Measurements in Grapevine: Cultivar and Water Status Matter. *Plants* **2023**, *12*, 2412. [CrossRef] [PubMed]
24. Taylor, J.A.; Acevedo-Opazo, C.; Pellegrino, A.; Ojeda, H.; Tisseyre, B. Can Within-Season Grapevine Predawn Leaf Water Potentials Be Predicted from Meteorological Data in Non-Irrigated Mediterranean Vineyards? *OENO One* **2012**, *46*, 221. [CrossRef]
25. Fares, A.A.; Vasconcelos, F.; Mendes-Moreira, J.; Ferreira, C. Predicting Predawn Leaf Water Potential up to Seven Days Using Machine Learning. In *Progress in Artificial Intelligence*; Marreiros, G., Melo, F.S., Lau, N., Lopes Cardoso, H., Reis, L.P., Eds.; Lecture Notes in Computer Science; Springer International Publishing: Cham, Switzerland, 2021; Volume 12981, pp. 39–50. [CrossRef]
26. Tosin, R.; Pôças, I.; Gonçalves, I.; Cunha, M. Estimation of Grapevine Predawn Leaf Water Potential Based on Hyperspectral Reflectance Data in Douro Wine Region. *VITIS-J. Grapevine Res.* **2020**, *59*, 9–18. [CrossRef]

27. Correa, J.; Dorta, P.; López-Díez, A.; Díaz-Pacheco, J. Analysis of Tropical Nights in Spain (1970–2023): Minimum Temperatures as an Indicator of Climate Change. *Int. J. Clim.* **2024**, *44*, 3006–3027. [CrossRef]
28. Choné, X. Stem Water Potential Is a Sensitive Indicator of Grapevine Water Status. *Ann. Bot.* **2001**, *87*, 477–483. [CrossRef]
29. Voce, S.; Škrab, D.; Vrhovsek, U.; Battistutta, F.; Comuzzo, P.; Sivilotti, P. Compositional Characterization of Commercial Sparkling Wines from Cv. Ribolla Gialla Produced in Friuli Venezia Giulia. *Eur. Food Res. Technol.* **2019**, *245*, 2279–2292. [CrossRef]
30. Comuzzo, P.; Marconi, M.; Zanella, G.; Querzè, M. Pulsed Electric Field Processing of White Grapes (Cv. Garganega): Effects on Wine Composition and Volatile Compounds. *Food Chem.* **2018**, *264*, 16–23. [CrossRef] [PubMed]
31. Loira, I.; Morata, A.; Comuzzo, P.; Callejo, M.J.; González, C.; Calderón, F.; Suárez-Lepe, J.A. Use of *Schizosaccharomyces pombe* and *Torulaspora delbrueckii* Strains in Mixed and Sequential Fermentations to Improve Red Wine Sensory Quality. *Food Res. Int.* **2015**, *76*, 325–333. [CrossRef] [PubMed]
32. Šuklje, K.; Baša Česnik, H.; Janeš, L.; Kmecl, V.; Vanzo, A.; Deloire, A.; Sivilotti, P.; Lisjak, K. The Effect of Leaf Area to Yield Ratio on Secondary Metabolites in Grapes and Wines of *Vitis vinifera* L. Cv. Sauvignon Blanc. *OENO One* **2013**, *47*, 83. [CrossRef]
33. Suklje, K.; Čuš, F. Modulation of Welschriesling Wine Volatiles through the Selection of Yeast and Lactic Acid Bacteria. *OENO One* **2021**, *55*, 245–260. [CrossRef]
34. Martelanc, M.; Slaghenaufi, D.; Radovanović Vukajlović, T.; Martin Rojas, D.A.; Suklje, K.; Sternad Lemut, M.; Mozetič Vodopivec, B.; Butinar, L.; Antalick, G. A Unique Mixture of Monoterpenes and Volatile Phenols Characterises Zelen Wine's Aromatic Profile. *OENO One* **2025**, *59*. [CrossRef]
35. Levin, A.D.; Deloire, A.; Gambetta, G.A. Does Water Deficit Negatively Impact Wine Grape Yield over the Long Term? *Tech. Rev.* **2020**. [CrossRef]
36. Guilpart, N.; Metay, A.; Gary, C. Grapevine Bud Fertility and Number of Berries per Bunch Are Determined by Water and Nitrogen Stress around Flowering in the Previous Year. *Eur. J. Agron.* **2014**, *54*, 9–20. [CrossRef]
37. Gambetta, G.A.; Herrera, J.C.; Dayer, S.; Feng, Q.; Hochberg, U.; Castellarin, S.D. The Physiology of Drought Stress in Grapevine: Towards an Integrative Definition of Drought Tolerance. *J. Expe. Bot.* **2020**, *71*, 4658–4676. [CrossRef] [PubMed]
38. Wang, Z.; Deloire, A.; Carbonneau, A.; Federspiel, B.; López, F. Study of Sugar Phloem Unloading in Ripening Grape Berries under Water Stress Conditions. *OENO One* **2003**, *37*, 213. [CrossRef]
39. Ojeda, H.; Andary, C.; Kraeva, E.; Carbonneau, A.; Deloire, A. Influence of Pre- and Postveraison Water Deficit on Synthesis and Concentration of Skin Phenolic Compounds during Berry Growth of *Vitis vinifera* Cv. Shiraz. *Am. J. Enol. Vitic.* **2002**, *53*, 261. [CrossRef]
40. De Oliveira, J.B.; Egipto, R.; Laureano, O.; De Castro, R.; Pereira, G.E.; Ricardo-da-Silva, J.M. Climate Effects on Physicochemical Composition of Syrah Grapes at Low and High Altitude Sites from Tropical Grown Regions of Brazil. *Food Res. Int.* **2019**, *121*, 870–879. [CrossRef] [PubMed]
41. Shahood, R.; Torregrosa, L.; Savoi, S.; Romieu, C. First Quantitative Assessment of Growth, Sugar Accumulation and Malate Breakdown in a Single Ripening Berry. *OENO One* **2020**, *54*, 1077–1092. [CrossRef]
42. Savoi, S.; Herrera, J.C.; Carlin, S.; Lotti, C.; Bucchetti, B.; Peterlunger, E.; Castellarin, S.D.; Mattivi, F. From Grape Berries to Wines: Drought Impacts on Key Secondary Metabolites. *OENO One* **2020**, *54*, 569–582. [CrossRef]
43. Diverres, G.; Fox, D.J.; Harbertson, J.F.; Karkee, M.; Keller, M. Response of Riesling Grapes and Wine to Temporally and Spatially Heterogeneous Soil Water Availability. *Am. J. Enol. Vitic.* **2024**, *75*, 0750019. [CrossRef]
44. Marais, J.; Van Wyk, C.J. Effect of Grape Maturity and Juice Treatments on Terpene Concentrations and Wine Quality of *Vitis vinifera* L. Cv. Weisser Riesling and Bukettraube. *S. Afr. J. Enol. Vitic.* **2017**, *7*, 26–35. [CrossRef]
45. Liu, H.; Cao, X.; Liu, X.; Xin, R.; Wang, J.; Gao, J.; Wu, B.; Gao, L.; Xu, C.; Zhang, B.; et al. UV-B Irradiation Differentially Regulates Terpene Synthases and Terpene Content of Peach. *Plant Cell Environ.* **2017**, *40*, 2261–2275. [CrossRef] [PubMed]
46. Koundouras, S.; Marinos, V.; Gkoulioti, A.; Kotseridis, Y.; Van Leeuwen, C. Influence of Vineyard Location and Vine Water Status on Fruit Maturation of Nonirrigated Cv. Agiorgitiko (*Vitis vinifera* L.). Effects on Wine Phenolic and Aroma Components. *J. Agric. Food Chem.* **2006**, *54*, 5077–5086. [CrossRef] [PubMed]
47. Bindon, K.A.; Dry, P.R.; Loveys, B.R. Influence of Plant Water Status on the Production of $C_{13}$-Norisoprenoid Precursors in *Vitis vinifera* L. Cv. Cabernet Sauvignon Grape Berries. *J. Agric. Food Chem.* **2007**, *55*, 4493–4500. [CrossRef] [PubMed]
48. Peyrot Des Gachons, C.; Leeuwen, C.V.; Tominaga, T.; Soyer, J.; Gaudillère, J.; Dubourdieu, D. Influence of Water and Nitrogen Deficit on Fruit Ripening and Aroma Potential of *Vitis vinifera* L Cv Sauvignon Blanc in Field Conditions. *J. Sci. Food Agric.* **2005**, *85*, 73–85. [CrossRef]
49. Lebon, E.; Dumas, V.; Pieri, P.; Schultz, H.R. Modelling the Seasonal Dynamics of the Soil Water Balance of Vineyards. *Funct. Plant Biol.* **2003**, *30*, 699. [CrossRef] [PubMed]
50. Pellegrino, A.; Lebon, E.; Voltz, M.; Wery, J. Relationships between Plant and Soil Water Status in Vine (*Vitis vinifera* L.). *Plant Soil* **2005**, *266*, 129–142. [CrossRef]
51. Feddes, R.A.; Hoff, H.; Bruen, M.; Dawson, T.; De Rosnay, P.; Dirmeyer, P.; Jackson, R.B.; Kabat, P.; Kleidon, A.; Lilly, A.; et al. Modeling Root Water Uptake in Hydrological and Climate Models. *Bull. Am. Meteor. Soc.* **2001**, *82*, 2797–2809. [CrossRef]

52. Riou, C.; Valancogne, C.; Pieri, P. Un Modèle Simple d'interception Du Rayonnement Solaire Par La Vigne-Vérification Expérimentale. *Agronomie* **1989**, *9*, 441–450. [CrossRef]
53. Schwartzman, M.; Zur, B. Emitter Spacing and Geometry of Wetted Soil Volume. *J. Irrig. Drain. Eng.* **1986**, *112*, 242–253. [CrossRef]